Center for Turbulence Research
Proceedings of the Summer Program 1990

On the subgrid-scale modeling of compressible turbulence

By Kyle Squires[1] AND Otto Zeman[1]

A new sub-grid scale model is presented for the large-eddy simulation of compressible turbulence. In the proposed model, compressibility contributions have been incorporated in the sub-grid scale eddy viscosity which, in the incompressible limit, reduce to a form originally proposed by Smagorinsky (1963). The model has been tested against a simple extension of the traditional Smagorinsky eddy viscosity model using simulations of decaying, compressible homogeneous turbulence. Simulation results show that the proposed model provides greater dissipation of the compressive modes of the resolved-scale velocity field than does the Smagorinsky eddy viscosity model. For an initial r.m.s. turbulence Mach number of 1.0, simulations performed using the Smagorinsky model become physically unrealizable (i.e., negative energies) because of the inability of the model to sufficiently dissipate fluctuations due to resolved scale velocity dilatation. The proposed model is able to provide the necessary dissipation of this energy and maintain the realizability of the flow. Following Zeman (1990), turbulent shocklets are considered to dissipate energy independent of the Kolmogorov energy cascade. A possible parameterization of dissipation by turbulent shocklets for Large-Eddy Simulation is also presented.

1. Introduction

Compressibility effects in turbulent flows depend mainly on the r.m.s. fluctuating Mach number, M_t, defined as the ratio of the r.m.s. fluctuating velocity to the mean field sonic velocity. Direct numerical simulations (DNS) of homogeneous turbulence indicate that, in general, the direct compressibility effects on turbulence are insignificant if $M_t = O(10^{-1})$ in the sense that the solenoidal (rotational) part of the fluctuating velocity field and the acoustic (irrotational) field are decoupled. The acoustic field, which is determined mainly by initial conditions, plays only a passive role in the overall turbulence dynamics (Blaisdell 1990, Zeman and Blaisdell 1990). Only when M_t exceeds a value of about 0.3 does compressibility begin to noticeably influence turbulence dynamics and structure. Further increase in M_t may lead to formation of shock-like structures or turbulent shocklets. Shocklet formation has been detected in the DNS of decaying turbulence when the initial value of M_t exceeded 0.5 (Lee, *et al.* 1990). In the DNS of homogeneous shear turbulence, Blaisdell (1990) detected shocklets for $M_t \geq 0.7$. Zeman (1990) suggested that weak shocklets may be responsible for the growth rate attenuation in shear layers and proposed a physical model for shocklet formation and the associated (dilatation) dissipation.

1 Center for Turbulence Research

On the basis of the DNS results and experimental evidence in mixing layers (e.g., Papamoschou and Roshko 1987), compressibility effects may be broadly classified by the magnitude of M_t. Thus, we shall refer to the range $0.3 < M_t < 0.6$ as moderate Mach numbers whereby the compressibility effects are observable but with no formation of shock-like structures (which signifies interactions between compressive (acoustic) and solenoidal fields). At larger Mach numbers, $M_t > 0.6$, a full scope of compressibility-induced effects may be expected, such as shocklet and baroclinic vorticity generation and significant solenoidal/compressive field interactions.

In large eddy simulation (LES) techniques, the r.m.s. velocity of subgrid-scale turbulence is smaller by the order $O(\triangle x/L)^{1/3}$ than that of the energy containing eddies of scale L. The lower limit on the mesh size $\triangle x$ is set by the computer. In the LES calculations presented later in section 4, $L/\triangle x \approx 30$, and it follows that the r.m.s. Mach number associated with subgrid scales is $(M_t)_{sg} = M_t(\triangle x/L)^{1/3} \approx 0.3M_t$. Thus, for realistic resolved-scale Mach numbers $M_t < 1$, the subgrid scale turbulence can be considered as incompressible but acted on by the large-scale compression and/or expansion and by inhomogeneities in the resolved thermal field as well. In section 2, we describe a formulation of a Smagorinsky-type SGS model which incorporates these compressibility contributions.

The possibility of occurrence of shocklets (at larger-than-moderate Mach numbers) presents a problem which must be treated separately from the SGS modeling. We can envisage that in the real flow a shocklet will have formed whose cross-section is sketched in figure 1. Because the shocklet is formed by the large-scale motions, it is expected to span an area of several mesh sizes, but since the shock thickness (λ_s) scales on viscosity, the gradients and dissipation associated with the shock front cannot be resolved in LES. It may be shown that the ratio $\lambda_s/\triangle x$ is proportional to $(\rho/\triangle\rho)(L/\triangle x)Re_L^{-1}$, where Re_L is the large scale (turbulent) Reynolds number and $\triangle\rho/\rho$ is a relative density jump across the shock. Because Re_L is arbitrarily large, λ_s will always be a negligible fraction of $\triangle x$ and, therefore, the actual shock front will be smeared over several mesh points and the shocklet dissipation underestimated by the order $O(\lambda_s/\triangle x)$ (Zeman 1990). The shocklet dissipation rate is locally very high and is independent of the Kolmogorov energy cascade and of the SGS turbulence. Therefore, it cannot be made a part of the SGS mode, and the only alternative is to represent the shocklet-induced effects by means of added (virtual) stresses in the resolved-scale governing equations. This approach is described in section 3. The LES numerical method is described in section 4, and computational results of LES of decaying compressible turbulence are presented in section 5. Section 6 concludes the report.

2. Large-scale compressibility effects on SGS energy and viscosity

The set of compressible LES equations obtained by Favre filtering the governing equations are

$$\frac{\partial\overline{\rho}}{\partial t} + \frac{\partial\overline{\rho}\widetilde{U}_i}{\partial x_i} = 0 \tag{1}$$

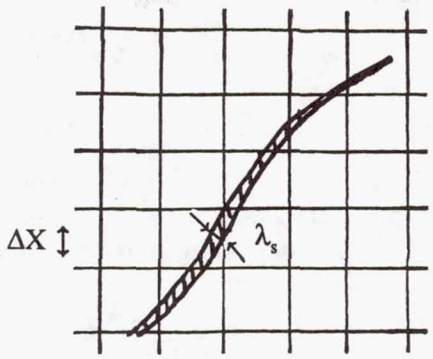

FIGURE 1. Schematic of a shocklet in a computational grid.

$$\frac{\partial}{\partial t}(\overline{\rho}\widetilde{U}_i) + \frac{\partial}{\partial x_j}(\overline{\rho}\widetilde{U}_j\widetilde{U}_i) = -\frac{\partial \overline{P}}{\partial x_i} + \frac{\partial \overline{\sigma}_{ij}}{\partial x_j} - \frac{\partial \tau_{ij}}{\partial x_j} \tag{2}$$

$$\frac{\partial}{\partial t}(\overline{\rho}\widetilde{E}) + \frac{\partial}{\partial x_j}(\overline{\rho}\widetilde{U}_j\widetilde{E}) = -\frac{\partial \overline{P}\widetilde{U}_j}{\partial x_j} + \frac{\partial \overline{U_i\sigma_{ij}}}{\partial x_j} + \frac{\partial}{\partial x_j}\left(\overline{\kappa\frac{\partial T}{\partial x_j}}\right) - \frac{\partial \pi_j}{\partial x_j} - \frac{\partial q_j}{\partial x_j} \tag{3}$$

$$\tau_{ij} = (\overline{\rho U_i U_j} - \overline{\rho}\widetilde{U}_i\widetilde{U}_j) \approx \overline{\rho}\widetilde{u_i u_j} \tag{4}$$

$$q_j = c_v(\overline{\rho T U_j} - \overline{\rho}\widetilde{T}\widetilde{U}_j) \approx c_v\overline{\rho}\widetilde{tu_j} \tag{5}$$

$$\pi_j = \overline{PU_j} - \overline{P}\widetilde{U}_j \approx \overline{pu_j} \tag{6}$$

Here, U_i, P, T are velocity, pressure, and temperature and $E = c_vT + U_jU_j/2$ is the total energy per unit mass. The viscous stress tensor is represented as σ_{ij} in equations (2) and (3). The field decomposition is $X = \widetilde{X} + x$, where $\widetilde{X} = \overline{\rho X}/\overline{\rho}$ is the filtered (resolved) quantity and, as opposed to incompressible flows, is obtained through Favre filtering. The sub-grid component of the variable X is denoted as x. The proposed Smagorinsky-type closures to the stress tensor τ_{ij} and heat flux q_j are

$$\frac{\tau_{ij}}{\overline{\rho}} = \widetilde{u_iu_j} = -2\nu_T S^*_{ij} + \frac{1}{3}q^2\delta_{ij} \tag{7}$$

$$\frac{q_i}{c_v\overline{\rho}} = \widetilde{tu_i} = -\alpha_{ij}\frac{\partial \widetilde{T}}{\partial x_j} \tag{8}$$

where

$$S^*_{ij} = \frac{1}{2}(\widetilde{U}_{i,j} + \widetilde{U}_{j,i} - \frac{2}{3}\nabla\cdot\widetilde{\mathbf{U}}\delta_{ij}) \tag{9}$$

is the trace-free strain rate tensor, $q^2 = \widetilde{u_ju_j}$ is (twice) the Favre-averaged kinetic energy of SGS turbulence, and ν_T and α_{ij} are, respectively, eddy viscosity and (tensor) eddy diffusivity due to SGS turbulence. Now our task is to parameterize

the effect of the resolved compressive field on the SGS viscosity and diffusivity in a functional form

$$\nu_T = \nu_{To} F(M_t, \nabla \cdot \tilde{\mathbf{U}}, \nabla T, \nabla P), \tag{10a}$$

$$\alpha_{ij} = Pr_t^{-1} \nu_{To} H_{ij}(M_t, \nabla \cdot \tilde{\mathbf{U}}, \nabla T, \nabla P), \tag{10b}$$

where $\nu_{To} \propto (\triangle x)^2 |S_{ij}|$ is the (Smagorinsky) viscosity, and Pr_t is the turbulent Prandtl number in the incompressible limit $M_t = 0$. Also, in this limit $F \to 1$, and $H_{ij} \to \delta_{ij}$. With the aid of the fluctuating part of the equation of state, the pressure-flux term $\pi_i = \overline{pu_i}$ can be expressed as

$$\pi_i = R(\overline{\rho} \widetilde{tu_i} + \tilde{T} \overline{\rho' u_i}). \tag{11}$$

As mentioned already, it is justified to treat the SGS turbulence as incompressible; therefore, π_i is negligible compared to either of the terms on the RHS of (11) and $\widetilde{tu_i}/T \approx -\overline{\rho' u_i}/\overline{\rho}$. In order to determine the functions F and H_{ij} in equations (10a) and (10b), we shall approximate the conservation equations for SGS turbulence energy q^2 and heat flux $\widetilde{tu_i}$ as in second-order closure schemes, with the resolved scale motions acting as the mean (input) field. Neglecting the third-order correlations, the transport equations for q^2 and $\widetilde{tu_i}$ may be expressed as (e.g., see Zeman 1990)

$$\frac{Dq^2}{Dt} = -2\widetilde{u_i u_j} S_{ij}^* - \frac{2}{3} q^2 \nabla \cdot \tilde{\mathbf{U}} - 2\overline{u}_j \frac{\partial \overline{P}}{\partial x_j} \frac{1}{\overline{\rho}} - 2\frac{q^3}{\Lambda} + \frac{2}{\overline{\rho}} \overline{p u_{j,j}} \tag{12}$$

$$\frac{D\widetilde{tu_i}}{Dt} = -\widetilde{u_i u_j} \frac{\partial \tilde{T}}{\partial x_j} - \widetilde{tu_j} \frac{\partial \tilde{U}_i}{\partial x_j} - C_h \widetilde{tu_i} \frac{q}{\Lambda}. \tag{13}$$

The average of the fluctuating velocity u_i is by definition, $\overline{u}_i = -\overline{\rho' u_i}/\overline{\rho}$ and according to (11) (with $\pi_i = 0$) it is approximated as $\overline{u}_i \approx \widetilde{tu_i}/\tilde{T}$. The fourth term in (12) represents the SGS solenoidal dissipation $\epsilon_s = q^3/\Lambda$; the dissipation scale Λ scales on the mesh size $\triangle x$ and will be determined later. The constant C_h in the heat flux equation (13) is the tendency-to-isotropy constant and its value is dictated by the Prandtl number Pr_t; typically, $C_h \approx 6.5$. Employing the inertial subrange relations, we find that the convective derivative terms in (12) and (13) are of order $O(\triangle x/L)^{2/3}$ smaller compared with the principal right-hand-side (RHS) terms and are neglected. Since the convective derivative terms are small and the sub-grid scale turbulence Mach number is also small, the last term in equation (12) representing the pressure dilatation correlation of the sub-grid scales may also be neglected. It should be remarked, however, that the convective-term discard may not be justified in the regions containing shock-like structures (see section 3).

In order to obtain expressions in the form (10), we shall recast (12) and (13) in terms of the SGS viscosity ν_T and write

$$\nu_T = \beta \Lambda q \tag{14}$$

where β is presently an undetermined constant. With the aid of (7) and (14), equations (12) and (13) can now be solved for ν_T, α_{ij}, q^2, and Pr_t. To first order in $\nabla \cdot \widetilde{\mathbf{U}}$ we obtain

$$q^2 = 2\beta\Lambda^2 \left|S^*_{ij}\right|^2 + \beta\Lambda^2 \frac{\nabla\overline{P}\cdot\nabla\widetilde{T}}{\overline{\rho}\widetilde{T}Pr_t} - \frac{\sqrt{2\beta}}{3}\Lambda^2 \left|S^*_{ij}\right| \nabla\cdot\widetilde{\mathbf{U}}, \tag{15}$$

and

$$\alpha_{ij} = \frac{\nu_T}{Pr_t}\delta_{ij} - \frac{\nu_T}{3}\frac{\Lambda}{q}S^*_{ij}. \tag{16}$$

As mentioned earlier, Pr_t is related to the tendency-to-isotropy constant C_h; from the second-order closure equations we obtain $Pr_t \approx C_h/8.12 = 0.8$ (Zeman 1990). The viscosity constant β in (14) must be such that in the incompressible limit $M_t = 0$, the SGS viscosity approaches a well-tested Smagorinsky value $\nu_{To} = (C_s\triangle x)^2|S^*_{ij}|$. The obvious choice here is $\Lambda = \triangle x$ and, hence, $\beta = C_s^{4/3}$. An accepted value for the Smagorinsky constant is $C_s = 0.2$, and this gives $\beta = 0.12$. A more accurate analysis, based on the inertial subrange relations (e.g. Tennekes and Lumley 1972), gives

$$\epsilon_s = \frac{q^3}{\Lambda} \approx \frac{q^3(k)k}{(2\alpha)^{3/2}}, \tag{17}$$

where $k \approx \pi/\triangle x$ is the smallest SGS wavenumber and $\alpha \approx 1.5$ is the Kolmogorov constant. From (17), $\Lambda = (2\alpha)^{3/2}\triangle x/\pi \approx 1.65\triangle x$ and then $\beta = 0.06$. Tests of the SGS model represented by the closure equations (7), (8), and (14)-(16) showed a reasonable insensitivity to the choice of β and, therefore, the results presented in this paper were obtained using $\Lambda = \triangle x$.

3. Virtual shocklet stresses

As mentioned earlier, in LES the information on shocklet occurrence is lost due to a lack of resolution, and the total energy dissipation is likely to be underestimated. The would-be shock front is numerically diffused and may manifest itself by numerical instability. Here, an approach is suggested to reconstruct the shocklet effects through inclusion of additional (virtual) stresses in the resolved scale equations. These virtual stresses depend on the local Mach number $m = (\widetilde{U}_j\widetilde{U}_j)^{1/2}/a(\widetilde{T})$, the density (or pressure) gradients, and possibly on molecular properties. The principal purpose of this stress reconstruction is to recover some part of the dissipation associated with the possible shock structures.

The idea of the virtual stress parameterization is based on the model and theory of shocklet dissipation developed by Zeman (1990) and on the assumption that although the actual-flow shock structure cannot be resolved in the LES, the actual and LES fields share statistical properties of energy containing motions. Thus, we assume that the actual (or DNS) and LES fields have the same pdf $p(m)$ of the fluctuating Mach number $m(\mathbf{x},t)$ and that the local density (or pressure) gradients and $\nabla\cdot\widetilde{\mathbf{U}}$ are, in combination with $m(\mathbf{x},t)$, sufficient indicators of an unresolved

shock event. Then, one of the plausible ways to express the virtual stress divergence due to an unresolved shocklet (to be added to the RHS of equation (2)) is

$$(\tau_{ij,j})_{shk} \propto -\nabla\overline{\rho}a^2(\frac{m^2-1}{m})^2 p_s(m, \nabla\cdot\widetilde{\mathbf{U}}, \nabla\overline{\rho}), \tag{18}$$

where $p_s(x,y,z)$ is a conditional, shock probability function which is an indicator of the virtual shock occurrence; the necessary but not sufficient condition for the shock occurrence is $m > 1$ and$\nabla\cdot\widetilde{\mathbf{U}} < 0$. According to (18) the shock stress divergence is in the direction of the density front $\nabla\overline{\rho}$, and we convince ourselves that equation (18) gives a correct magnitude of shocklet dissipation by forming the kinetic energy equation for the resolved scales, $K = \widetilde{U}_j\widetilde{U}_j/2$. With $(\tau_{ij,j})_{shk}$ added to the RHS of (2), we obtain

$$\frac{DK}{Dt} = -((\tau_{ij})_{shk}\widetilde{U}_i)_{,j} + (\tau_{ij})_{shk}\widetilde{U}_{i,j} + \text{ other terms.} \tag{19}$$

The (dilatation) dissipation due to the virtual shocklet is the second term in (19) and with (18) we obtain

$$\frac{DK}{Dt} \propto +\nabla\cdot\widetilde{\mathbf{U}}\overline{\rho}a^2(\frac{m^2-1}{m})^2 p_s(m, \widetilde{\mathbf{U}}, \nabla\overline{\rho}) = -\epsilon_{shk}. \tag{20}$$

Note that the differential operation is not to be applied to the scalar function in m and to p_s, since these serve only as rescaling and probability measures.

The proposed parameterization of shocklet dissipation in LES will have to be verified by comparing DNS of shocklet turbulence with a corresponding LES field. The comparison might be difficult to interpret in nonstationary (decaying) turbulence simulations. To this end, we shall attempt in the future to generate a stationary turbulence field at sufficiently high r.m.s. Mach number by random forcing applied at the largest scales.

As a final point, we should keep in mind that the large-scale shock front may have a significant effect on the (presently neglected) convective terms in the kinetic energy budget of SGS turbulence (12). Since the average velocity $\widetilde{U}_s$ normal to the shock front must be of the order of the sonic speed a, then the advective derivative $\widetilde{U}_j q^2_{,j}$ in (12) could be of order $aq^2/\triangle x$ and, therefore, larger than the primary terms such as the dissipation $\epsilon_s \propto q^3/\triangle x$. Inclusion of these shock front advection effects in the SGS models has not so far been considered.

4. Simulation methods and parameters

The Favre-filtered equations for a compressible fluid (equations 1-3) were solved for the case of temporally evolving homogeneous turbulence. Since homogeneous turbulence is in principle unbounded, numerical simulation of these flows employ periodic boundary conditions in a finite computational domain. The application of periodic boundary conditions typically permits extremely accurate schemes for

the evaluation of spatial derivatives. In the numerical method used for the present work, spatial derivatives are evaluated using high-order accurate compact finite differences. These difference schemes possess spectral-like resolution (see Lele 1990), and the formal order of accuracy of the scheme used in the present work is sixth order. The discretized equations were solved using 32^3 grid points and were time advanced using a third-order Runge Kutta method.

It should be remarked that the filtered momentum and energy equations shown in section 2 contain terms which may not be greatly simplified following the filtering of the governing equations. For example, no appreciable simplification of the viscous stresses in the momentum equations or the viscous dissipation terms in the energy equation is obtained by filtering equations (2) and (3). In fact, since the energy of the flow is computed using the transport equation for *total* energy, a number of additional terms arise following the filtering operation. It is important to remember, however, that many of these terms, e.g., the viscous dissipation terms in the energy equation, are negligible at high Reynolds numbers (at least away from solid boundaries). Other terms are assumed to be represented by the sub-grid scale model.

The initial conditions for all simulations were identical to those used by Lee, *et al.* (1990), i.e., the initial velocity field is constrained to be divergence free, and there are no initial density or temperature fluctuations. The velocity fluctuations were also constructed from an initial energy spectrum of the form

$$E(k) = Ak^4 \exp\left[-2(k/k_0)^2\right]. \tag{21}$$

Simulations were performed using the SGS model shown in section 2 and compared to results obtained using an 'incompressible' Smagorinsky-type model, i.e., a sub-grid scale model neglecting corrections for resolved-scale velocity dilatation. This model will be referred to as the Smagorinsky model and is summarized below

$$\frac{\tau_{ij}}{\overline{\rho}} = -2\nu_T S^*_{ij} + \frac{1}{3} q^2 \delta_{ij}, \tag{22}$$

$$\frac{q_i}{c_v \overline{\rho}} = -\alpha_{ij} \frac{\partial T}{\partial x_j} \tag{23}$$

where

$$\nu_T = \sqrt{2\beta^3}\Lambda^2 \left|S^*_{ij}\right|, \tag{24}$$

$$\alpha_{ij} = \frac{\nu_T}{Pr_t}\delta_{ij} - \frac{\nu_T}{3}\frac{\Lambda}{q} S^*_{ij}, \tag{25}$$

and

$$q^2 = 2\beta\Lambda^2 \left|S^*_{ij}\right|^2. \tag{26}$$

As mentioned in section 2, the value of the constant β was determined by considering an incompressible limit, i.e., the limit which yields the Smagorinsky model shown above. Following this limit process, the value of the constant β used for the

simulations presented in this paper was 0.12. The reader is referred to section 6 for further discussion considering determination of the constant. This value of β corresponds to a value of the Smagorinsky constant, C_s, of 0.2. It is should be remarked, however, that a value of $C_s = 0.2$ is larger than the value of 0.092 determined by Erlebacher, *et al.* (1990). Erlebacher, *et al.* determined the constant from direct numerical simulations of compressible homogeneous turbulence by correlating exact and modelled stresses.

The remaining parameter for the sub-grid scale model is the value of the turbulent Prandtl number, Pr_t. As shown in section 2, Pr_t is related to the tendency-to-isotropy constant, C_h. Using the second-order closure equations, a value of $Pr_t = 0.8$ is then obtained. Alternatively, one can also show that filtering the pressure-work term in the energy equation gives rise to an additional sub-grid scale heat flux (i.e., other than that arising from filtering the convective terms). This additional flux augments the overall SGS heat flux by a factor of γ. If the ratio of the sub-grid scale fluxes of momentum and heat are considered to be the same as in incompressible turbulence, then the turbulent Prandtl number for compressible turbulence must then be reduced by a factor of γ. A widely accepted value of Pr_t for simulations of incompressible turbulence is 0.7. Accounting for the reduction of Pr_t by the additional sub-grid scale heat flux from the pressure-work term, the value of the turbulent Prandtl number for compressible turbulence is then $Pr_t = 0.5$. It is interesting to note that this value is the same as that determined by Erlebacher, *et al.* (1990) using their DNS database. No tests were conducted in the present study to investigate the influence of Pr_t on the computed flow fields, and a value of $Pr_t = 0.5$ was used for the results presented in section 5.

Since the initial density and temperature fields were considered to be uniform and the initial velocity field was solenoidal, the properties of the initial fields may be specified by the Taylor-microscale Reynolds number, Re_λ $(= u'\lambda/\nu)$, and the turbulence Mach number, M_t. The values of M_t for the three cases investigated in the present work were 0.61, 0.8, and 1.0. The corresponding values of the Taylor-microscale Reynolds number were 50, 65, and 83. For each of these Mach numbers, simulations were performed using both the Smagorinsky eddy viscosity model and the proposed model that incorporates additional terms representing the effect of compressibility.

5. Results

Shown in figure 2 is the time development of twice the resolved-scale turbulence energy for an initial turbulence Mach number of 0.8. The time axis in figure 2, as well as figure 4, has been made dimensionless by the eddy turnover time, τ_e, in the initial field. The two curves shown in figure 2 correspond to the Smagorinsky eddy viscosity model and the proposed model which incorporates corrections due to resolved scale compressibility. As is evident from the figure, there is negligible difference between the resolved-scale energy obtained using either the Smagorinsky model or the proposed model. This result is consistent with that obtained at the lower turbulence Mach number, $M_t = 0.61$.

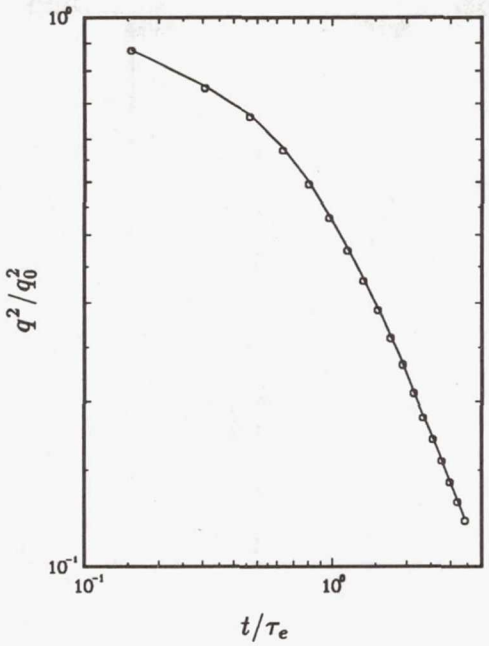

FIGURE 2. Time development of turbulence kinetic energy for an initial $M_t = 0.8$. ——— , Smagorinsky; o , proposed.

Shown in figures 3a and 3b are the radial energy spectra of the velocity and dilatation fields at $t/\tau_e = 1.3$ for an initial $M_t = 0.8$. Consistent with the results observed in figure 2, it can be seen from figure 3a that there is negligible difference between the velocity spectrum obtained using either sub-grid scale model. Figure 3b shows, however, that there is greater energy in the resolved-scale dilatation field at higher wavenumbers from the computation using the Smagorinsky model than for the proposed model. Figures 3a and 3b clearly show that the model more significantly affects the compressive modes of the velocity as opposed to the solenoidal velocity components.

The time development of the resolved-scale turbulence energy is shown in figure 4 for both the Smagorinsky and proposed models for an initial $M_t = 1.0$. As was also observed for the lower Mach number cases, this figure shows that at early times, the resolved scale energy is virtually identical for both cases. It was also found, however, that the flow field becomes physically unrealizable using the Smagorinsky model. The solid line in figure 4 has been drawn up to the instant in time in which the resolved-scale temperature becomes negative.

The radial energy spectra of the resolved scale velocity at the time step immediately preceding the instant at which the flow field computed using the Smagorinsky model becomes unrealizable has been shown in figure 5a. It may be observed from this figure that the spectra of the velocity fields obtained using both the Smagorinsky and proposed model are virtually identical. The mean-square energy obtained by integrating the spectra were found to differ by only 0.06 percent. The spectra of

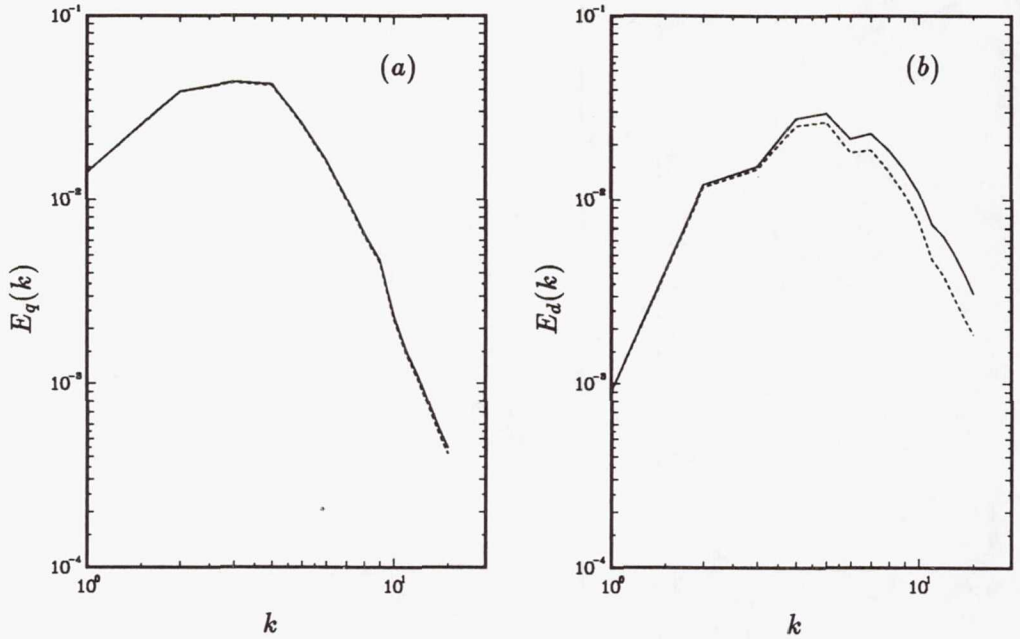

FIGURE 3. Radial spectra at $t/\tau_e = 1.3$ of (a) velocity, and (b) dilatation for an initial $M_t = 0.8$. ——— , Smagorinsky; ---- , proposed.

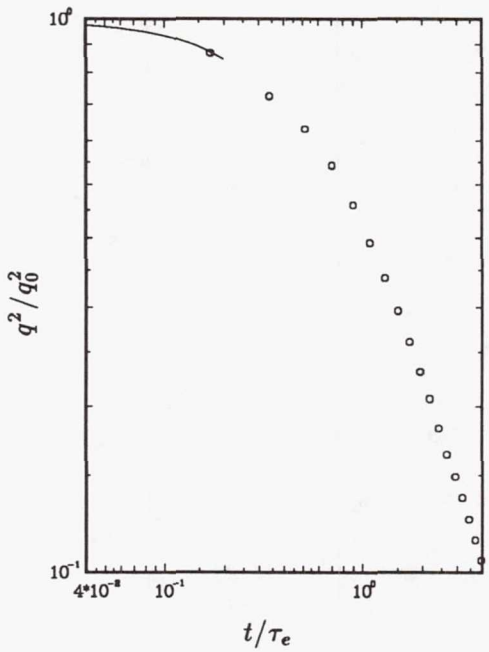

FIGURE 4. Time development of turbulence kinetic energy for an initial $M_t = 1.0$. ——— , Smagorinsky; o , proposed.

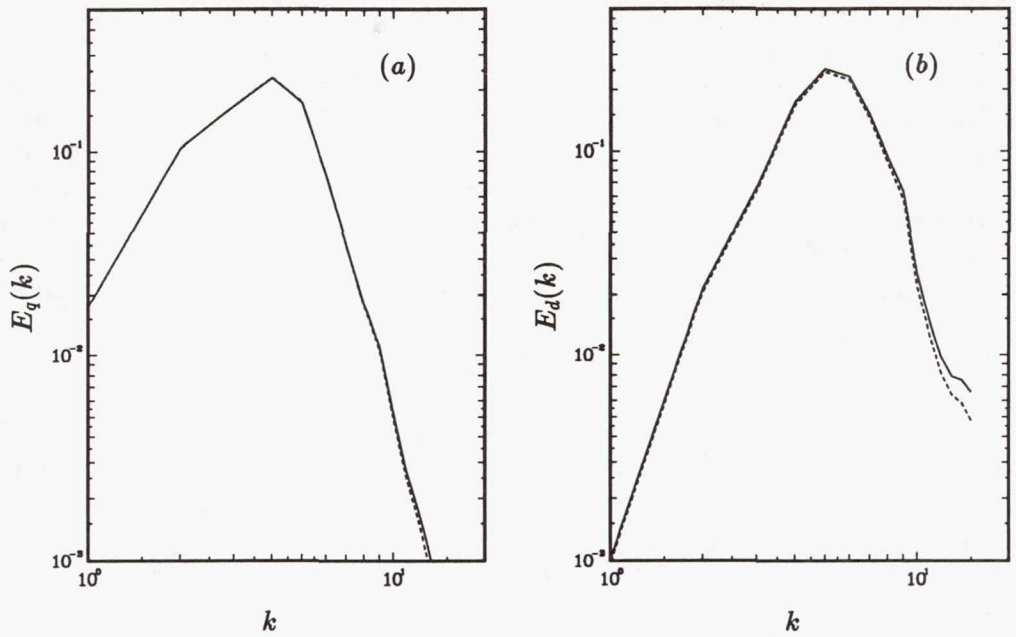

FIGURE 5. Radial spectra at $t/\tau_e = 0.2$ of (a) velocity, and (b) dilatation for an initial $M_t = 1.0$. ——— , Smagorinsky; - - - - , proposed.

the resolved-scale dilatation field is shown in figure 5b. As could also be observed in the dilatation spectra from the $M_t = 0.8$ case, the dilatation spectra obtained using the proposed model is below that of the Smagorinsky model at the higher wavenumbers. The mean-square, resolved-scale dilatation at this instant in time differs by approximately 6 percent for simulations performed using the two models. This excess in the dilatation field obtained using the Smagorinsky model is sufficient to cause the flow field to become physically unrealizable. Locally, dilatation fluctuations can become extremely large. The proposed model provides sufficient dissipation in these regions to prevent the resolved-scale temperature from becoming negative. These results also illustrate that the differences in the resolved scales obtained using the two models occur primarily in the high-wavenumber end of the spectrum. It is precisely in this region in which resolved-scale compression and expansion are most significant.

6. Summary and future work

A new sub-grid scale model for the Large-Eddy Simulation of compressible turbulence has been developed and tested using numerical simulations of temporally-evolving compressible turbulence. The development of the model was guided by concepts employed in second-order closure modeling of compressible turbulence. The proposed model reduces to Smagorinsky's (1963) model for the LES of incompressible turbulence in the limit $M_t \to 0$ and also requires only one adjustable constant. The constant is determined from the incompressible limit in which case it must reduce to a value widely used in LES of incompressible turbulence ($C_s \approx 0.2$).

Simulation results obtained using both the proposed model as well as the Smagorinsky model showed that at turbulence Mach numbers of 0.61 and 0.8 there is negligible difference between the resolved scale solenoidal velocity fields obtained using either model. For an initial $M_t = 1.0$, it was found that the Smagorinsky model was unable to provide sufficient dissipation in regions of large compression and/or expansion. This inability to provide the necessary dissipation in these regions in turn caused the flow to become physically unrealizable (i.e., negative temperature). The proposed model, which incorporates the effect of large-scale velocity dilatation, does provide the necessary dissipation in these regions and maintains the physical realizability of the flow.

While the usefulness of the proposed model over the Smagorinsky model has been demonstrated at high turbulence Mach numbers, important issues remain to be resolved. The effect of shocklet dissipation was not incorporated into the sub-grid scale model for the simulation results presented in this report. Before incorporating the virtual shocklet stress (see section 3) into the simulations, the parameterization should first be verified by correlating modelled shocklet dissipation against actual shocklet dilatational dissipation. As was mentioned in section 3, such a comparison may be difficult to interpret in simulations of decaying turbulence. To alleviate this difficulty, one may apply a body force at the largest scales of the flow in order to obtain a quasi-stationary state. An advantage of applying an external body force is that it is possible to maintain a reasonably steady value of the turbulence Mach number. Comparison of the shocklet stress from simulations of compressible turbulence which has been artificially forced at the largest scales should be more meaningful than that obtained from decaying turbulence. Such an effort will be undertaken in the near future.

Another issue to be resolved is the effect of Reynolds number on the simulation results. All of the results presented in this report were obtained from simulations which included molecular effects, i.e., finite Reynolds number. Thus, the role of the eddy viscosity was to primarily provide the extra dissipation needed in regions of high dilatation. Since the philosophy behind LES is to compute high-Reynolds number turbulent flow fields the model should be tested in simulations at infinite Reynolds number, i.e., zero molecular viscosity and thermal conductivity. Such simulations will provide a more rigorous test of the proposed model as well as better demonstrate differences between the proposed model and the Smagorinsky model.

Finally, a new sub-grid scale model has been presented by Germano, Piomelli, Moin, and Cabot during this summer program which does not require an *a priori* choice of the model constant(s) and also allows backscatter from the small to the large scales. The formulation of the model is based upon an algebraic identity between the subgrid-scale stresses at two different levels and the resolved filtered stresses. This formulation is general enough so that it may be applied to the LES of compressible turbulence. Therefore, another direction of future work will be to incorporate the proposed model presented in this paper with the dynamic sub-grid scale model presented by Germano, *et al.*

REFERENCES

BLAISDELL, G. A. 1990 Numerical simulations of compressible homogeneous turbulence. Ph.D. dissertation, Department of Mechanical Engineering, Stanford University, Stanford, California.

ERLEBACHER, G., HUSSAINI, M. Y., SPEZIALE, C. G., & ZANG, T. A. 1990 Toward the Large-Eddy Simulation of compressible turbulent flows. *ICASE report 90-76.*

LEE, S., LELE, S. K., & MOIN, P. 1990 Eddy shocklets in decaying compressible turbulence. *Physics of Fluids.* in press.

LELE, S. K. 1990 Compact finite difference schemes with spectral-like resolution. *CTR Manuscript 107.* also submitted to the Journal of Computational Physics.

PAPAMOSCHOU, D. & ROSHKO, A. 1987 The compressible turbulent shear layer: an experimental study. *J. Fluid Mech.* **197,** 453.

SMAGORINSKY, J. 1963 General circulation experiments with the primitive equations. *Monthly Weather Review.* **93,** 99.

TENNEKES, H. L., & LUMLEY, J. L. 1972 *A first course in turbulence.* The MIT press.

ZEMAN, O., & BLAISDELL, G. A. 1990 New physics and models for compressible turbulence. to appear in *Advances in Turbulence.* Springer-Verlag.

ZEMAN, O. 1990 Dilatation dissipation: the concept and application in modeling compressible mixing layers. *Physics of Fluids.* **2,** 178-188.